

Autonomous undulatory serpentine locomotion utilizing body dynamics of a fluidic soft robot

Cagdas D Onal^{1,2} and Daniela Rus¹

¹ Computer Science and Artificial Intelligence Laboratory, Massachusetts Institute of Technology, Cambridge, MA 02139, USA

² Mechanical Engineering Department, Worcester Polytechnic Institute, Worcester, MA 01609, USA

E-mail: cdonal@wpi.edu

Received 30 November 2012


Accepted for publication 27 February 2013

Published 25 March 2013

Online at stacks.iop.org/BB/8/026003

Abstract

Soft robotics offers the unique promise of creating inherently safe and adaptive systems. These systems bring man-made machines closer to the natural capabilities of biological systems. An important requirement to enable self-contained soft mobile robots is an on-board power source. In this paper, we present an approach to create a bio-inspired soft robotic snake that can undulate in a similar way to its biological counterpart using pressure for actuation power, without human intervention. With this approach, we develop an autonomous soft snake robot with on-board actuation, power, computation and control capabilities. The robot consists of four bidirectional fluidic elastomer actuators in series to create a traveling curvature wave from head to tail along its body. Passive wheels between segments generate the necessary frictional anisotropy for forward locomotion. It takes 14 h to build the soft robotic snake, which can attain an average locomotion speed of 19 mm s⁻¹.

 Online supplementary data available from stacks.iop.org/BB/8/026003/mmedia

(Some figures may appear in colour only in the online journal)

1. Introduction

Robots of today are heavily utilized in factory automation. These machines provide perfect solutions in terms of speed, precision and controllability to repetitive and limited number of tasks in controlled environments at a safe distance from human beings, but are less capable and unsafe for human-centered tasks. In natural environments, the traditional rigid robotic architecture causes significant performance losses due to limited adaptability in the hardware that cannot be easily compensated by the software. Part of this problem is the lack of flexibility in conventional actuation mechanisms.

Soft robotics provides an alternative. Given their small minimum stiffness, soft mechanisms are inherently safe and adaptive. A soft body can deform and absorb energy in the case of a crash, and conform to unknown objects and conditions. These inherent advantages bring soft robots closer to biological

capabilities observed in nature. We consider these properties as an embedded form of intelligence in the mechanics of the body. This integration of the mechanical response into the computation system is a type of morphological computation [1, 2]. A soft robot can adapt and deform to keep contact with uneven ground for operation in unstructured environments. Similarly, soft robots are more suitable for human interaction as they pose minimal risk for injury in assistance applications such as helping the elderly or incapacitated in fundamental tasks including raising up from the bed or reaching objects on the floor. In the long run, we envision wearable soft robotic systems such as a smart glove to help reduce physical impairments like hand tremors in everyday tasks while causing minimal motion constraints for the wearer.

There has been a flurry of recent studies in soft robotics focusing on building functional soft actuators and systems. A miniature 3D pneumatic rubber actuator is described in [3].



Figure 1. Experimental prototype of the fluidic elastomer robotic snake. The body consists of four bidirectional fluidic elastomer actuators in series. Valves and passive wheels are attached between segments. The electronics and energy supply are inside the tail on the right.

This actuator has a cylindrical outer shell and a segmented inner shell to achieve bending and axial deformations. Another rubber actuator has a pleated structure [4], which can generate rotary motion. It is suitable for rehabilitation applications and designed to replace conventional linear pneumatic actuators.

At the system level, [5, 6] demonstrated a promising soft crawling mobile robot. This robot has many potential applications, but it is ultimately tethered, which limits its functionality. With a different approach, [7] describes a bio-inspired robotic platform based on an octopus arm. The arm is made up of silicone rubber and driven with embedded tendons. It can locomote by pushing, and grasp objects similar to its biological counterpart. A soft robotic caterpillar is introduced in [8] that can quickly curl into a wheel and roll away as part of a bio-inspired escape response.

Nevertheless, the current state of soft robotics has significant drawbacks. New actuation technologies are crucial in the emergence of soft robotics. The soft robots in existence mainly utilize two kinds of actuation: electrical and fluidic [9, 10]. Electrical approaches tend to introduce constraints such as large electrical fields [11] or ionic substrates [12]. Fluidic power is promising for this application, as it offers a large energy density and simple mechanism of actuation. However, fluidic approaches require additional valving hardware for control [13], and an on-board pressure source for tetherless implementation [14–16].

In previous work, we have shown two different approaches to create autonomous soft pneumatic mobile robots, utilizing a chemical reaction to generate gas for a self-rolling robot [15], and miniature CO₂ cartridges for a fish robot [16]. Our prior research described the actuation and power components for soft robots without demonstrating the use of the components within fully autonomous soft robotic systems.

In this work, we propose a third approach to achieve tetherless soft locomotion using fluidic power: a miniature compressor on a bio-inspired robotic system. More specifically, this work presents an autonomous self-contained soft robotic snake with on-board actuation power, pressure regulation, valving and computation. A prototype of this robot is shown in figure 1.

To our knowledge, this is the first self-contained fluidic soft snake robot. The advantage of a soft actuation scheme

for autonomous navigation with robotic snakes is that the segments do not create discrete angles with each other, but rather curve with uniform angular change approaching continuum behavior. We show that the robotic snake in this paper can generate a traveling wave of curvature from head to tail with only feedforward valve open or close commands [17], utilizing the static and dynamic responses of fluidic elastomer actuators. Similar to its biological counterpart, the soft robotic snake undulates autonomously at a measured mean locomotion velocity of 19 mm s⁻¹. It takes 14 h to build this robot in our lab from scratch using pre-fabricated molds.

2. Methods

2.1. Snake locomotion

Snake locomotion is well studied in the robotics community because it is an efficient form of crawling locomotion in natural environments without the complexity of limb motions [18]. Snakes achieve this by anisotropic frictional properties of their skin [19, 20]. Friction forces in the normal direction of the body axis are larger than those along the body. A recent review of snake-like robots is given in [21].

This special frictional behavior in conjunction with a traveling sinusoidal wave in curvature κ along the body written as

$$\kappa(s, t) = \alpha \cos(2\pi(s + t/T)) \quad (1)$$

creates forward propulsion, where $s \in [0, 1]$ is the normalized arc length of the body neutral axis, α is the amplitude and T is the period of the wave [19].

Starting with Hirose's work on the active cord mechanism [18], researchers developed different kinds of snake robots to synthesize the elegant and unique locomotion capabilities of these animals, which seem to glide effortlessly on granular terrain. These robots primarily have a serial kinematic linkage structure with no fixed base.

Locomotion is achieved with two main approaches. First can be described as a chain of active two-wheeled non-holonomic mobile robots [21]. In this case, the body joint actuation provides steering capability. The second and more interesting approach is converting the body joint actuation into net forward locomotion utilizing a frictional anisotropy with

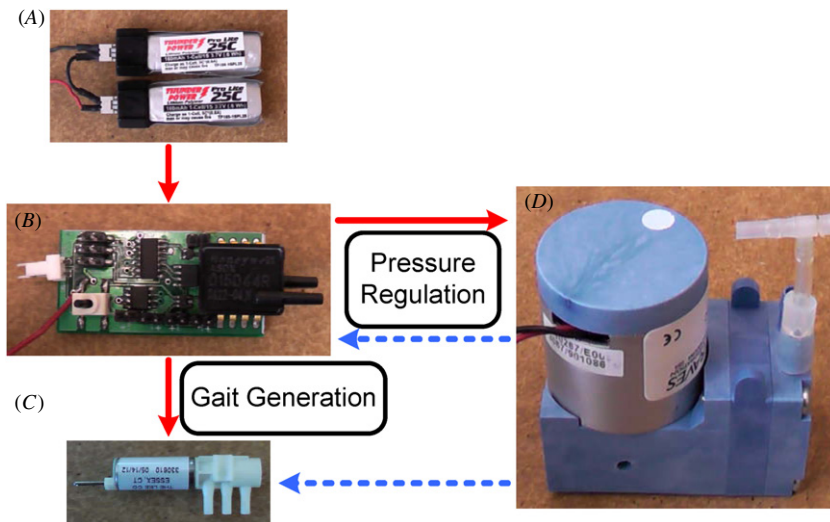


Figure 2. Soft snake architecture. The system is composed of (A) two miniature lithium polymer batteries for electrical energy, (B) a custom printed circuit board for pressure regulation and gait generation, (C) eight solenoid latching valves to address and actuate each side of the four segments and (D) a miniature compressor to convert electrical energy to pressure.

the ground [18]. The necessary frictional conditions are usually achieved by utilizing either passive wheels or skates.

In this work, we follow the second approach since it is similar to how biological snakes locomote. The valve-holders between segments also provide a natural place to attach passive wheels to create frictional anisotropy. Note that passive wheels provide a good solution to generate frictional anisotropy, but they offer limited utility in the types of natural environments we envision for our robotic snake. This design decision is motivated by the need to decouple the problems of developing a soft robotic snake and achieving frictional anisotropy with the soft body. Our main focus in this work is on solving the more general problem of realizing serpentine locomotion with a segmented fluidic elastomer actuation system. Our future work will include the development of a soft snake skin inspired by the biological counterpart to enable the same frictional properties without wheels or other rigid mechanisms.

2.2. System architecture

The soft robotic snake shown in figure 1 comprises four bidirectional fluidic elastomer actuators (FEAs) composed in series to create segments that autonomously undulate similar to its biological counterpart. All the electrical and rigid elements are placed together at the tail and valves are placed between segments along the length of the body. The robot is 280 mm long, 32 mm tall and 12 mm wide.

Figure 2 displays a pictorial description of the general architecture of the soft robotic snake. Electrical energy from two miniature lithium polymer batteries (Thunder Power TP160-1SPL25) is used to power the electronics and converted to mechanical actuation energy by the on-board compressor. An on-board custom printed circuit board with an Atmel ATtiny24 microcontroller continuously monitors the pressure supply using a gauge pressure sensor (Honeywell ASDX 030G24R) and keeps it at a relatively constant value using a bang-bang controller. This actuation energy is distributed to the

four body segment FEAs by switching between two miniature latching solenoid valves (Lee Company) to actuate both directions of each FEA. Locomotion is achieved by a specific sequencing of valve commands. The result is a traveling wave of curvature following a serpentine gait algorithm. The discrete nature of the solenoid valves provides step inputs to the actuators, which are smoothed by the actuator dynamics to approximate a sinusoidal wave necessary for this type of locomotion.

The body of the robot is a serial composition of four bidirectional FEAs. It is molded from silicone rubber in three parts from custom 3D printed molds by extending the fabrication process detailed in [22] to four actuators. Two of the molds create meandering fluidic channels and the third mold embeds an inextensible constraint in a long and thin solid elastomer strip. The first two molds are then glued on both sides of the third mold to seal the fluidic channels and create one continuous body with four actuation segments. Passive wheel and valve holders are 3D printed and placed between the actuation segments along the body. The tail enclosure is 3D printed and the electronics hardware is inserted. Finally, two sets of wheels are attached to the tail for balance.

2.3. Fluidic elastomer bending actuators

In previous work, we derived a physical static model of out-of-plane displacement for bending-type FEAs [15]. This model relates the pressure input to output displacement, using the geometric and material properties of the actuators. We find this model to be very useful in the design of FEAs for different requirements.

The operational principle behind our design for FEAs relies on using pressure for actuation. In an elastomeric substrate, the expansion of embedded fluidic channels due to pressure input creates overall deformation of the actuator. By the inclusion of appropriate physical constraints, this deformation is forced to follow a desired bending

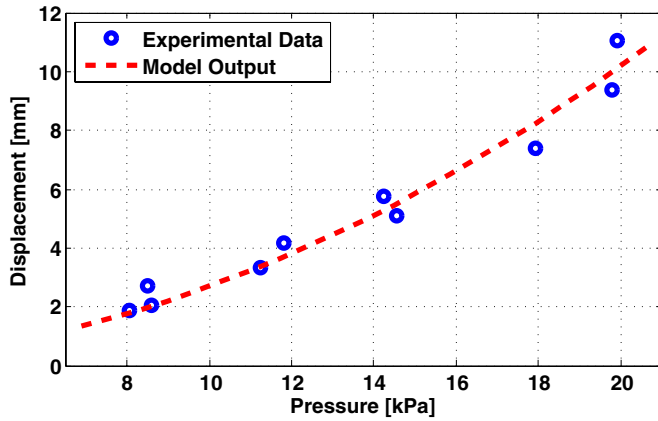


Figure 3. Out-of-plane displacement of a fluidic elastomer actuator versus the measured pressure input. Hollow blue circles are experimental data. The dashed curve is the model output. The nonlinearity in this curve stems from the stress–strain relationship of the polymer.

displacement. Parallel rectangular fluidic channels reside inside an elastomeric film. The channels are connected on two ends in a meandering arrangement. Without any constraints, the material tends to undergo tensile deformation. With an inextensible thin layer sandwiched by channels on both sides, we can convert this axial deflection to a bidirectional out-of-plane bending motion. The bending response of an FEA prototype is shown in [22].

Applied pressure P inside the rectangular channels with height h_c and length l_c creates axial stresses σ_x in the material with height h_t and length l_t given as

$$\sigma_x = P \frac{h_c}{h_t - h_c}. \quad (2)$$

The resulting strain $\epsilon_x(\sigma_x)$ is a nonlinear function of the induced stresses. The inextensible sheet constitutes the neutral axis of bending in the composite. Thus, the total bending angle θ can be calculated from the contributions of each channel as

$$\theta = 2n \arctan \frac{l_c \epsilon_x(\sigma_x)}{2h_c}. \quad (3)$$

The curvature κ for this actuator is then

$$\kappa = \theta/l_t = \frac{2n}{l_t} \arctan \frac{l_c \epsilon_x(\sigma_x)}{2h_c}. \quad (4)$$

The experimental deflection response of a silicone rubber FEA for pressure inputs ranging from 1 to 3 psi (6.9 to 20.7 kPa) is depicted in figure 3 with the corresponding simulation results according to the given model shown by the dashed curve. The stress–strain relationship of the material is determined by a power function fit to the experimental true stress and strain data.

A static model is useful to describe the response of the actuators for long timescales or low frequencies, but it fails to take the transients into account. Since it is more suitable to use miniature solenoid valves that can only switch between on and off states compared to larger analogue flow control valves, we have to harness the dynamics of the actuators to achieve an approximately sinusoidal curvature response over time.

We can derive a dynamic model using electrical circuit equivalence. Fluidic tubing and channels act as impedances

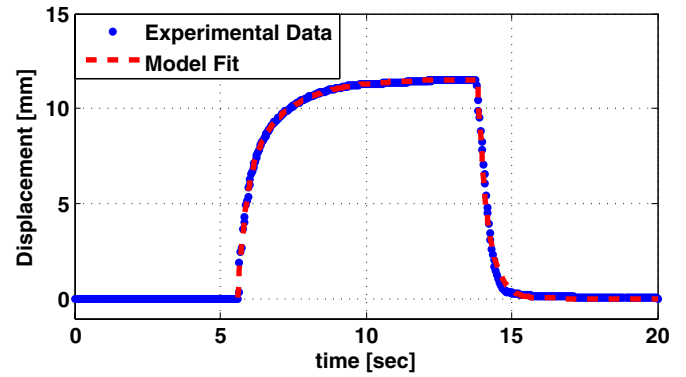


Figure 4. Experimental data of out-of-plane displacement of a fluidic elastomer actuator with respect to time. Separate second-order differential equations are fitted to the actuation and venting phases. This model provides accurate representation of the motion dynamics.

and fluidic chambers act as capacitances, which enables a second-order differential equation to fundamentally describe the motion dynamics of FEAs as shown in figure 4. This figure displays experimental data of out-of-plane displacement, using external image processing of a calibrated camera feed of an FEA clamped on one end, as a function of time for a constant inlet pressure of $P_{in} = 20.7$ kPa.

A solution to the second-order ordinary differential equation is

$$\delta = C_o + C_1 \exp(-t/\tau_1) + C_2 \exp(-t/\tau_2), \quad (5)$$

where δ is the out-of-plane displacement of the actuator, C_i , $i \in [0, 2]$ are constant coefficients and τ_k , $k \in 1, 2$ are the dynamic time constants [22]. The maximum δ_{max} value that the deflection curve converges is analytically predicted by the static model and fitting the dynamic equation to the experimental data yields the necessary parameters to accurately describe the transient response of the actuators for a step input.

2.4. Control

The on-board control board has two main functions. First, it needs to keep the pressure input to the actuators at an approximately constant value. To do this, it can turn the compressor on and off at a high bandwidth. Since a compressor can only increase the pressure, and there is no reason to reduce the compression rate by a proportional term, we use a bang-bang controller for this task. The basic algorithm is then to build up pressure at the maximum compression rate until a given threshold value is exceeded. After this point, the compressor is turned fully off until the pressure gets below this threshold. We found that this basic controller works very well for our requirements, intermittently turning the compressor on to keep the pressure relatively constant during robot locomotion.

The second function of the microcontroller is to generate the undulation gait for a given oscillation period. Position control of low bandwidth soft systems is not a trivial problem. Any given continuous curvature function can be generated by switching valves on and off at a high frequency similar to

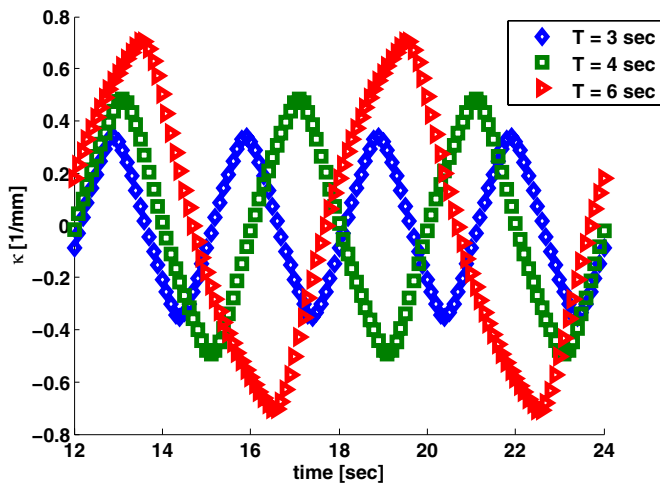


Figure 5. Simulation of a bidirectional FEA segment using a square wave pressure input signal with three different period values. Actuator dynamics smooths the input signal to approximate a sinusoidal output curvature. Smaller period values result in closer approximations with the expense of smaller amplitudes for the same pressure amplitude.

a pulse width modulation approach, but this requires many sensors and a complicated control scheme. As a result, in this work, we decided to harness the slow dynamics of our soft actuators to convert an electrical square wave input to a mechanical sinusoidal output. This is a good example of embodied intelligence of a soft robot helping simplify the burden on the control system.

Our approach is to use a feedforward controller that switches between two antagonistic actuators on both sides of each segment based on the sign of the target curvature. The segment dynamics, in turn, smooths these steps into a continuous function that approximates the necessary sinusoidal waveform, without the need for sensors, and more complicated feedback control implementations. Figure 5 shows an analysis of the dynamic response of these actuators for different switching period values ranging from 3 to 6 s. In this analysis, we used a constant pressure input that yields a maximum curvature value of 1 mm^{-1} in steady state according to the static model.

This figure shows that as the period decreases, the response becomes closer to a pure sinusoidal, but the amplitude also decreases. We determined that oscillation periods smaller than 3 s yield very small oscillation amplitudes. While it is possible to use a larger pressure input to increase the amplitude, this may also harm the actuators over time. On the other hand, increasing the period improves the amplitude but the waveform starts to lose its approximation of a sine-wave as the period becomes larger than 6 s. Therefore, we decided to use switching periods in this range for experiments.

Finally, the serpentine gait requires a traveling wave of curvature between the body segments. The soft robotic snake approaches continuum behavior but it still has a segmented structure. Since (1) is given for a continuous system, we need to discretize it as

$$\kappa_i(t) = \alpha \cos(2\pi(i/n_s + t/T)), \quad (6)$$

where κ_i is the curvature of the i th segment and $n_s = 4$ is the number of segments. The controller keeps track of the target curvature values of each segment to actuate one side of the i th segment for positive values of κ_i and the other side for $\kappa_i < 0$.

2.5. Soft robotic snake model

A soft linkage has different kinematics than traditional rigid chains. This difference is due to the inherent compliance of the body and the actuation principle. Made of a series of bidirectional bending modules, these robots approach a continuum behavior with increasing number of segments. In consequence, the final shape of the robot can be described by a continuous function and each point along the length of the linkage can be calculated from this function. The theory we present in this section can be applied to a general soft kinematic chain in a 2D implementation that represents our soft robotic snake design.

Traditional rigid kinematics models use joint angles as the basic input and the position and orientation of the tip end-effector as the output. For our soft chain, we will instead use the curvature of each segment as the independent variable. Since the input pressure to each segment has a direct effect on the curvature, this is appropriate. The resulting analysis yields a linear model similar to conventional rigid kinematics, with the exception that it is based on curvature information.

We develop the forward kinematics for our soft linkages using the following ideas. Given a bidirectional bending module i of length l_i , out of n modules in series, the normalized arc length $s_i \in [0, 1]$ and a curvature value κ_i , the orientation of this module can be written as

$$\theta_i = \kappa_i s + \theta_i(0), \quad (7)$$

where $\theta_i(0) = \theta_{i-1}(1)$ from continuity and $\theta_1(0) = \theta_0$ is the initial orientation of the kinematic chain base. The position of each point along the length of the module, in turn, is given as

$$x_i = \int l_i \cos \theta_i ds = \frac{l_i}{\kappa_i} \sin(\kappa_i s + \theta_i(0)) + x_i(0) - \frac{l_i}{\kappa_i} \sin \theta_i(0), \quad (8)$$

$$y_i = \int l_i \sin \theta_i ds = \frac{-l_i}{\kappa_i} \cos(\kappa_i s + \theta_i(0)) + y_i(0) + \frac{l_i}{\kappa_i} \cos \theta_i(0), \quad (9)$$

where $x_i(0) = x_{i-1}(1)$ and $y_i(0) = y_{i-1}(1)$ for continuity, and $x_1(0) = x_0$ and $y_1(0) = y_0$ indicate the initial position of the kinematic chain base. By stitching these equations for all n segments, we can accurately model each point along the soft linkage. Note that this model yields undefined results for $\kappa_i = 0$, which we compensate by substituting a small value for zero curvature values as $\kappa_i = \epsilon$ in our simulations.

Since this soft kinematic chain is not fixed to a base like a manipulator arm, to accurately describe its locomotion by undulation, we decouple the internal kinematics defined above from the external forces due to the frictional constraints [19]. By taking the vector sum of all frictional forces acting on each segment that result from a traveling curvature wave, we can

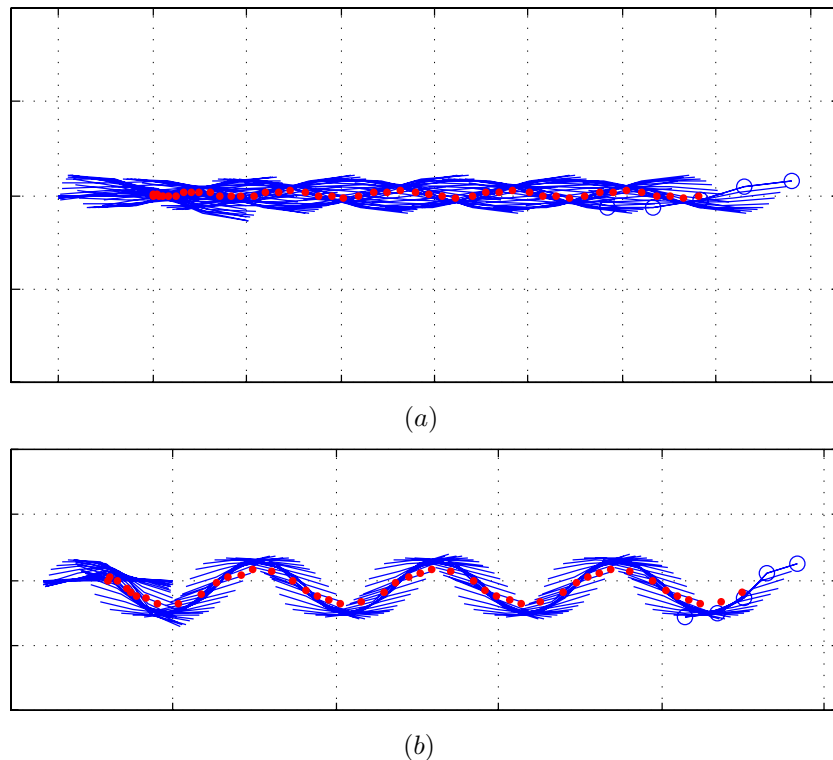


Figure 6. Non-dimensional simulation results of a soft robotic snake with four segments of unit length and unit mass. A series of body shapes and positions over time are overlaid to represent the motion history of the robot. The trajectory of the center-of-mass is represented as a red curve. Two main modes of locomotion are displayed: (a) a lower amplitude small period mode ($T = 4$ s, $\kappa_{\max} = 0.6$) and (b) a higher amplitude large period mode ($T = 6$ s, $\kappa_{\max} = 1$).

evolve a virtual base position following the ideas in [23]. To calculate the frictional forces we use a Coulomb model, with different coefficients for the normal and longitudinal directions at each segment.

Simulation results demonstrating the locomotion of a soft snake robot are displayed in figure 6. In these simulations, we used a soft robotic snake comprising four segments of unit length and mass. Friction coefficients in the normal ($\mu_n = 0.5$) and longitudinal ($\mu_l = 0.04$) directions are empirically chosen to simulate the required frictional anisotropy for each segment.

The simulations take a traveling square wave input, which represents the switching valve states, with a given period and amplitude, which represents the pressure input. Using the full segment dynamics, the square wave is smoothed to approximate a sinusoidal curve. The resulting shape generates external friction forces at points of contact with the ground. The vector sum of all the external forces, in turn, is used to move the base position of the body to complete an iteration.

Figure 6 displays two crawling locomotion modes. The top figure shows a low-amplitude, small period mode, where the robot tries to move fast with a small amplitude, resulting in considerable side slippage. This mode creates a motion history that resembles the interference pattern of two waves. The bottom figure displays a high-amplitude, large period mode, where the body undulates slowly with a larger period, to better track a single curve, similar to natural snakes.

3. Results and discussion

The snapshots of a locomotion experiment of the soft robotic snake taken in 2 s intervals are displayed in figure 7. This is an earlier prototype of the robot with off-board electronics and valving to demonstrate the proof-of-concept of soft fluidic serpentine locomotion. In this experiment, the gait algorithm is realized on an Arduino board using an external valve array. The robot traversed 18.4 ± 4 mm between each snapshot in this experiment, resulting in a net forward locomotion speed of 9.2 mm s^{-1} on average for an undulation period of 10 s.

A tethered mobile robot is essentially an oxymoron. Useful properties of a fluidic soft robot cannot be fully utilized if it has to be powered or controlled by an external source [5, 6]. A fundamental focus of this work is to lift this limitation by incorporating the necessary hardware on the body. The result is an autonomous self-contained soft robot. A similar locomotion experiment with this autonomous implementation is shown in figure 8. In this experiment, we used an input pressure of 25.1 kPa and an undulation period of 6 s.

While adding the tail enables autonomous operation, it may also introduce a potential issue where the rigid tail does not follow the same trajectory as the rest of the body, yielding changes in performance. Our preliminary tethered implementation does not have this issue as the whole body contributes to locomotion. To quantify the locomotion performance of the autonomous soft robotic snake, we used a Vicon motion capture system. In these experiments, we tracked

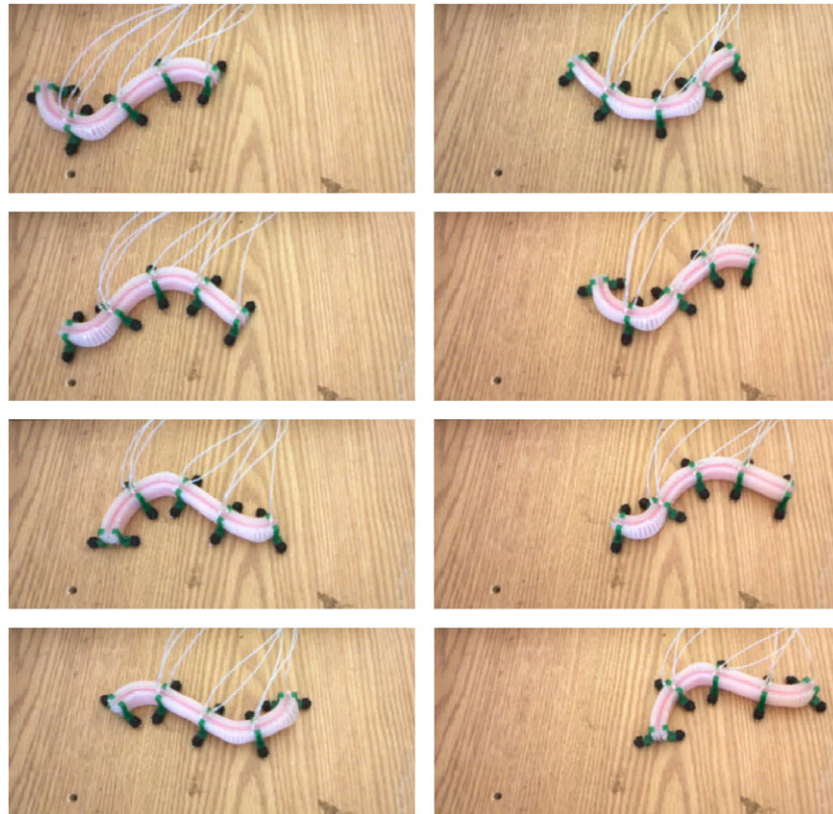


Figure 7. A tethered soft snake prototype undergoing lateral undulation with a period of 10 s, using a traveling sinusoidal curvature wave over its length. Snapshots are taken in equal time intervals of 2 s.

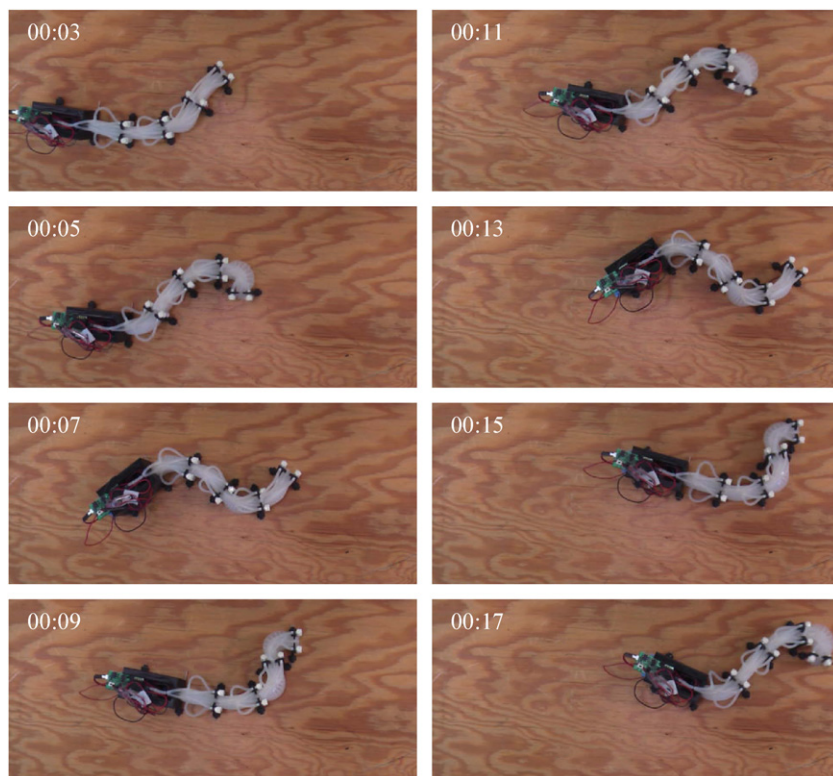


Figure 8. The soft snake prototype undergoing lateral undulation with a period of 6 s, using a traveling sinusoidal curvature wave over its length. Snapshots are taken in equal time intervals of 2 s.

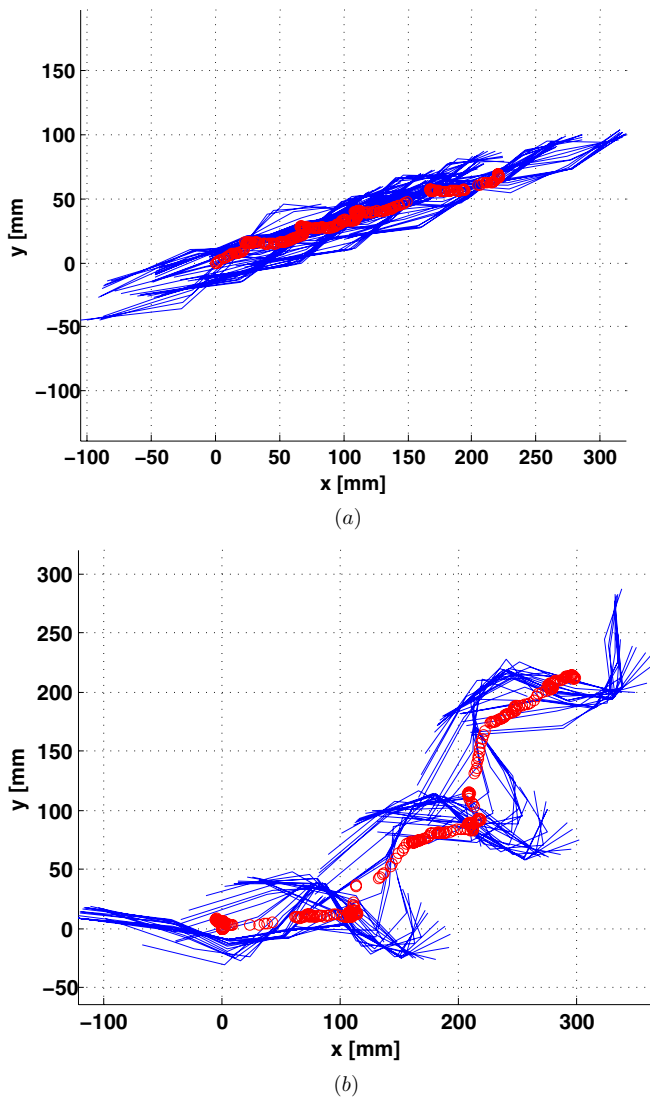


Figure 9. Results of motion capture experiments on the autonomous self-contained soft robotic snake. A series of body shapes and positions over time are overlaid to represent the motion history of the robot. The trajectory of the center-of-mass is represented as a red curve. Two main modes of locomotion are observed: (a) a lower pressure small period mode ($T = 4$ s, $P = 22.55$ kPa) and (b) a higher pressure large period mode ($T = 6$ s, $P = 27.65$ kPa).

the tail, each valve holder located between segments, and the head position over time. Figure 9 displays sample locomotion data of two experiments with different input pressure and undulation period values over 16.67 s time intervals. These figures show the position of the tracked points along the length of the robot over time, where the earlier positions are overlaid on the same figure to indicate the general locomotion pattern. The mean position of all the tracked points are also displayed to show the trajectory of the center of mass.

These figures display two main crawling locomotion behaviors we observed from this robot prototype, as predicted by the simulations. Figure 9(a) shows the low-pressure, small period mode, which does not create a large enough amplitude to track a single continuous trajectory as natural snakes do. Due to a lot of side slippage, the robot instead switches between two body waves that are of opposite phase to crawl forward. As

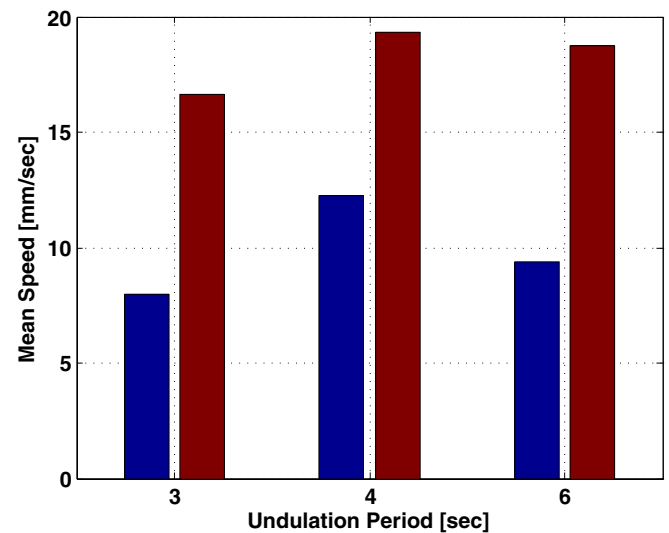


Figure 10. Experimental investigation of the average speed of the fluidic soft robotic snake for different combinations of the two parameters (input pressure P and undulation period T). Blue and red bars represent lower and higher pressure values, respectively ($P = 22.55$ kPa and $P = 27.65$ kPa).

Table 1. Comparison of the effect of different gait parameters on the locomotion speed of the soft snake.

T	P	
	22.55 kPa (3.27 psi)	27.65 kPa (4.01 psi)
3 s	7.98 ± 1.23 mm s ⁻¹	16.62 ± 3.24 mm s ⁻¹
4 s	12.27 ± 2.07 mm s ⁻¹	19.34 ± 2.12 mm s ⁻¹
6 s	9.4 ± 1.37 mm s ⁻¹	18.72 ± 3.31 mm s ⁻¹

previous body shapes and positions are overlaid on the same figure, this locomotion mode results in a ‘braided’ trajectory similar to an interference pattern of two waves. The losses due to side slippage also render this locomotion mode less efficient, yielding an average net locomotion speed of 12.27 mm s⁻¹ (0.04 body lengths (BL) per second).

In the second mode, with higher pressure inputs and larger undulation periods, the body approximately tracks a single wave as shown in figure 9(b). This mode results in a snake-like locomotion behavior that is also more efficient due to less side slippage, even though the undulation period is larger, to generate an average net locomotion speed of 18.72 mm s⁻¹ (0.07 BLs⁻¹). However, since we do not have control on the direction of the robot presently, the larger amplitude of undulation causes the heading to be less stable, amplifying the errors due to small inconsistencies in fabrication.

To better investigate the effect of changing the two main parameters, the input pressure P and the undulation period T , we performed systematic experiments. We analyzed all combinations of two safe input pressure values ($P = 22.55$ kPa and $P = 27.65$ kPa) and three undulation period values ($T = 3$ s, $T = 4$ s, and $T = 6$ s) to test the performance of the robot quantified by the average net locomotion speed. The results of this analysis are displayed in figure 10 and tabulated in table 1 with standard deviation values.

From this analysis, it is clear that for maximum speed, there is an optimal undulation period value for a given pressure input. This value seems to reside between $T = 3$ s and $T = 6$ s for both of the tested pressure inputs, based on the bending dynamics of the segments. We hypothesize that this value is at the point when the locomotion behavior switches from a multiple-body-wave crawling mode to a single-wave serpentine locomotion mode and heavily depends on the dynamics of the FEA segments. As the period is increased above this point, the robot loses speed as it spends extra time creating a larger amplitude body wave with a smaller net forward speed.

4. Conclusion

In this work, we presented a fluidic approach to creating soft mobile robots that offer inherent safety and adaptability. These robots are based on pressure-operated actuation modules called fluidic elastomer actuators (FEAs). These actuators are elastomer elements with embedded fluidic channels that undergo bending deformation when pressurized. Our focus was on a soft robotic snake comprised of four bidirectional FEAs composed in series. This robot was developed to synthesize the interesting locomotion gait of snakes in a soft robotic system. Approaching continuum behavior, the body compliance of this robot can provide a solution for some of the challenges of current actuation and transmission technology.

The result was a completely self-contained soft mobile robot, which does not require to be tethered to an electrical or pressure source. This was achieved by a tail that encompasses batteries, computation elements and energy conversion hardware to be complemented with valves and passive wheels distributed along the length of the robot. Embedded control was handled by an on-board microcontroller that regulated pressure input at a set constant value to the actuation units and generated the timings for the locomotion gait algorithm.

Building up on our prior results, we used the relatively slow dynamics of these soft actuators to our advantage, reducing the burden on the control system. We believe that this is a key property of soft robotics, the embodied intelligence in the mechanics.

The current prototype does not have steering capabilities, which is the subject of future work. Our approach to enable steering will be built on top of the current gait algorithm by adjusting the switching timings of the valves for each segment.

As is common in the robotic snake literature, we employed passive wheels in our work since they provide a good solution to generate frictional anisotropy. Nevertheless, passive wheels offer limited utility in the types of natural environments we envision for our robotic snake. This design decision is motivated by the need to decouple the problems of developing a soft robotic snake and achieving frictional anisotropy with the soft body. Our main focus in this work is on solving the more general problem of realizing serpentine locomotion with a segmented fluidic elastomer actuation system. Our future work will include the development of a soft snake skin inspired by the biological counterpart to enable the same frictional properties without wheels or other rigid mechanisms.

In general, we pursue research in many directions of soft robotics. We wish to improve our low-energy latching valves [13] to embed them inside FEA modules. We are working on a plug-and-play chemomechanical pressure generator [15], which has the potential to replace other pressure sources. Finally, we would like to expand our knowledge on the soft snake to build a soft manipulator arm. Future work in this area includes embeddable soft sensors, bio-inspired whole body manipulation techniques and obstacle negotiation.

Acknowledgments

The authors are grateful to Dr Ross Knepper for his help in the motion capture experiments. This work was supported by National Science Foundation (NSF) grants CCF-1138967 and NSF-1226883.

References

- [1] Pfeifer R, Iida F and Bongard J 2005 New robotics: design principles for intelligent systems *Artif. Life* **11** 99–120
- [2] Hauser H, Ijspeert A J, Füchslin R M, Pfeifer R and Maass W 2011 Towards a theoretical foundation for morphological computation with compliant bodies *Biol. Cybern.* **105** 355–70
- [3] Lianzhi Y, Yuesheng L, Zhongying H and Jian C 2010 Electro-pneumatic pressure servo-control for a miniature robot with rubber actuator *ICDMA: Int. Conf. on Digital Manufacturing and Automation* vol 1 pp 631–34
- [4] Ivlev O 2009 Soft fluidic actuators of rotary type for safe physical human machine interaction *IEEE 11th Int. Conf. on Rehabilitation Robotics* pp 1–5
- [5] Shepherd R F, Ilievski F, Choi W, Morin S A, Stokes A A, Mazzeo A D, Chen X, Wang M and Whitesides G M 2011 Multigait soft robot *Proc. Natl Acad. Sci.* **108** 20400–3
- [6] Morin S A, Shepherd R F, Wai Kwok S, Stokes A A, Nemiroski A and Whitesides G M 2012 Camouflage and display for soft machines *Science* **337** 828–32
- [7] Calisti M, Giorelli M, Levy G, Mazzolai B, Hochner B, Laschi C and Dario P 2011 An octopus-bioinspired solution to movement and manipulation for soft robots *Bioinspir. Biomim.* **6** 036002
- [8] Lin H T, Leisk G G and Trimmer B 2011 GoQBot: a caterpillar-inspired soft-bodied rolling robot *Bioinspir. Biomim.* **6** 026007
- [9] Albu-Schaffer A, Eiberger O, Grebenstein M, Haddadin S, Ott C, Wimbock T, Wolf S and Hirzinger G 2008 Soft robotics *IEEE Robot. Autom. Mag.* **15** 20–30
- [10] Trivedi D, Rahn C D, Kier W M and Walker I D 2008 Soft robotics: biological inspiration, state of the art, and future research *Adv. Bionics Biomech.* **5** 99–117
- [11] Keplinger C, Kaltenbrunner M, Arnold N and Bauer S 2010 Rontgens electrode-free elastomer actuators without electromechanical pull-in instability *Proc. Natl Acad. Sci.* **107** 4505–10
- [12] Bar-Cohen Y 2004 *Electroactive Polymer EAP Actuators as Artificial Muscles: Reality, Potential and Challenges* 2nd edn (Bellingham, WA: SPIE Optical Engineering Press)
- [13] Marchese A, Onal C D and Rus D 2011 Soft robot actuators using energy-efficient valves controlled by electropermanent magnets *IROS: IEEE/RSJ Int. Conf. on Intelligent Robots and Systems* pp 756–61
- [14] Kazerooni H 2005 Design and analysis of pneumatic force generators for mobile robotic systems *IEEE/ASME Trans. Mechatronics* **10** 411–8

- [15] Onal C D, Chen X, Whitesides G M and Rus D 2011 Soft mobile robots with on-board chemical pressure generation *ISSR: Int. Symp. on Robotics Research*
- [16] Marchese A D, Onal C D and Rus D 2012 A self-contained soft robotic fish: on-board pressure generation and embedded electro-permanent magnet valves *Int. Symp. on Experimental Robotics*
- [17] Ijspeert A J, Crespi A, Ryzcko D and Cabelguen J M 2007 From swimming to walking with a salamander robot driven by a spinal cord model *Science* **315** 1416–20
- [18] Hirose S 1993 *Biologically Inspired Robots: Snake-Like Locomotion and Manipulators* (Oxford: Oxford University Press)
- [19] Hua D L, Nirodya J, Scotta T and Shelleya M J 2009 The mechanics of slithering locomotion *Proc. Natl Acad. Sci.* **106** 10081–5
- [20] Guo Z V and Mahadevan L 2008 Limbless undulatory propulsion on land *Proc. Natl Acad. Sci.* **105** 3179–84
- [21] Hopkins J K, Spranklin B W and Gupta S K 2009 A survey of snake-inspired robot designs *Bioinspir. Biomim.* **4** 021001
- [22] Onal C D and Rus D 2012 A modular approach to soft robots *BioRob '12: 4th IEEE RAS & EMBS Int. Conf. on Biomedical Robotics and Biomechatronics* pp 1038–45
- [23] Liljeback P, Stavdahl O and Pettersen K Y 2008 Modular pneumatic snake robot: 3d modelling, implementation and control *Modelling Identif. Control* **29** 21–28